PHILOSOPHICAL TRANSACTIONS OF THE ROYAL SOCIETY A

Phil. Trans. R. Soc. A (2007) **365**, 1607–1625
doi:10.1098/rsta.2007.2034
Published online 12 April 2007

Designing bistable [2]rotaxanes for molecular electronic devices

By William R. Dichtel[1,2], James R. Heath[2,*] and J. Fraser Stoddart[1,*]

[1]*California NanoSystems Institute and Department of Chemistry and Biochemistry, University of California at Los Angeles, 405 Hilgard Avenue, Los Angeles, CA 90095, USA*
[2]*Division of Chemistry and Chemical Engineering, California Institute of Technology, 1200 East California Boulevard, Pasadena, CA 91125, USA*

The development of molecular electronic components has been accelerated by the promise of increased circuit densities and reduced power consumption. Bistable rotaxanes have been assembled into nanowire crossbar devices, where they may be switched between low- and high-conductivity states, forming the basis for a molecular memory. These memory devices have been scaled to densities of 10^{11} bits cm^{-2}, the 2020 node for memory of the International Technology Roadmap for Semiconductors. Investigations of the kinetics and thermodynamics associated with the electromechanical switching processes of several bistable [2]rotaxane derivatives in solution, self-assembled monolayers on gold, polymer electrolyte gels and in molecular switch tunnel junction devices are consistent with a single, universal switching mechanism whose speed is dependent largely on the environment, as well as on the structure of the switching molecule. X-ray reflectometry studies of the bistable rotaxanes assembled into Langmuir monolayers also lend support to an oxidatively driven mechanical switching process. Structural information obtained from Fourier transform reflection absorption infrared spectroscopy of rotaxane monolayers taken before and after evaporation of a Ti top electrode confirmed that the functionality responsible for switching is not affected by the metal deposition process. All the considerable experimental data, taken together with detailed computational work, support the hypothesis that the tunnelling current hysteresis, which forms the basis of memory operation, is a direct result of the electromechanical switching of the bistable rotaxanes.

Keywords: supramolecular chemistry; molecular electronics; bistable rotaxanes; switching; molecular memory; nanofabrication

1. Interlocked molecules in molecular electronic devices

'Bottom-up' approaches to the fabrication of molecular electronic devices (MEDs) are likely to become increasingly important as a means of overcoming the fundamental limitations of 'top-down' lithographic techniques. In the context

* Authors and address for correspondence: California Nanosystems Institute and Department of Chemistry and Biochemistry, University of California at Los Angeles, 405 Hilgard Avenue, Los Angeles, CA 90095-1569, USA (heath@chem.ucla.edu; stoddart@chem.ucla.edu).

One contribution of 12 to a Discussion Meeting Issue 'Supramolecular nanotechnology for organic electronics'.

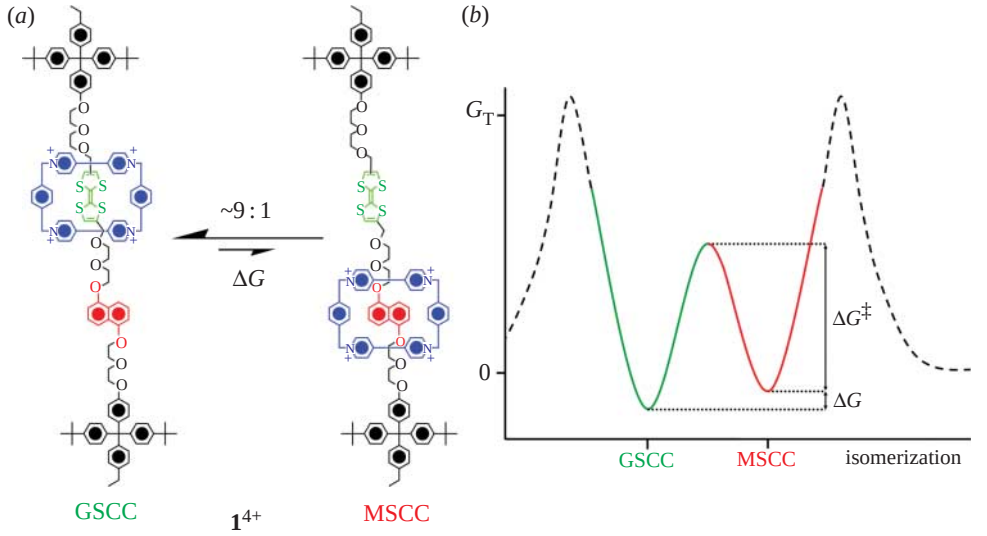

Figure 1. (*a*) The equilibrium associated with the translational isomerization of the bistable [2]rotaxane $\mathbf{1}^{4+}$ showing the interconversion between the ground-state co-conformation (GSCC) and the metastable state co-conformation (MSCC). (*b*) The potential energy surface for the isomerization showing the local minima corresponding to the GSCC and MSCC. The free energy difference for the $CBPQT^{4+}$ ring associated with the tetrathiafulvalene unit in reference to the 1,5-dioxynaphthalene one is indicated by ΔG, whereas the barrier to relaxation from the MSCC to the GSCC is denoted by $\Delta G^{\ddagger}$.

of this potentially changing agenda, the use of molecules as the passive and active components in devices promises ultimate scalability, minimal power consumption and low fabrication costs. Over the past few years, we have tapped into the advances in supramolecular chemistry (Lehn 1995) and template-directed synthesis (Anelli *et al.* 1992; Tseng & Stoddart 2002) to come up with a successful design of electrochemically switchable bistable [2]catenanes (Balzani *et al.* 2000) and [2]rotaxanes (Bissell *et al.* 1994; Tseng *et al.* 2004*a*). These molecular switches, based on mechanically interlocked and movable components, have been fabricated into nanowire crossbar arrays, producing working defect-tolerant memory devices of unprecedented densities. This article highlights the development of these molecular memory devices and the extensive experimental and theoretical investigations of the structure and mechanism of their operation in a variety of different chemical environments. Although the scope of this article is limited to the discussion of bistable [2]rotaxanes, bistable [2]catenanes have also been successfully incorporated and switched in the molecular switch tunnel junctions (MSTJs; Collier *et al.* 2000, 2001; Diehl *et al.* 2003).

2. Bistable [2]rotaxanes: structures and switching

The bistable redox-switchable [2]rotaxanes that have been used in MSTJs consist of a tetracationic cyclophane, cyclobis(paraquat-*p*-phenylene) ($CBPQT^{4+}$), with its two π-electron-deficient bipyridinium units, encircling a linear rod component

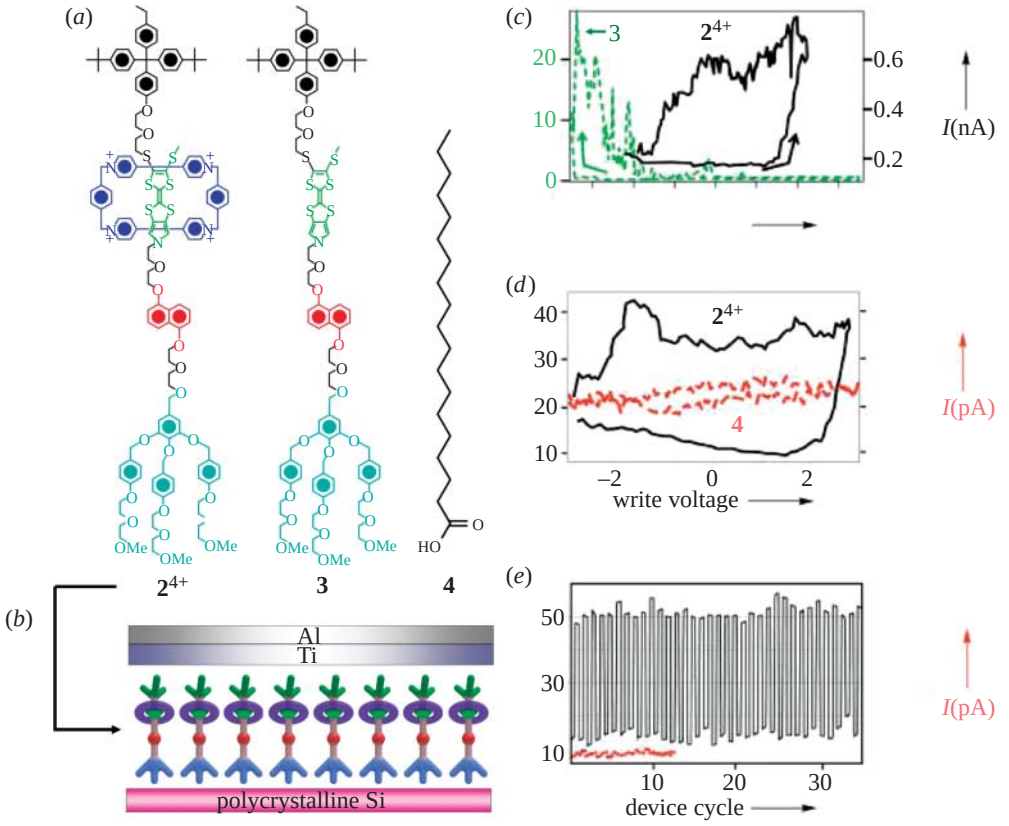

Figure 2. (*a*) MSTJ devices have been fabricated from the amphiphilic bistable [2]rotaxane $\mathbf{2}^{4+}$, the control dumb bell compound **3**, and the simple control, eicosanoic acid **4**. (*b*) The MSTJ device consists of a molecular monolayer sandwiched between a polycrystalline Si bottom electrode and a Ti/Al top electrode. (*c*) The remnant molecular signatures of $\mathbf{2}^{4+}$ (black) and **3** (green) recorded in micrometre-sized MSTJ devices. (*d*) The remnant molecular signatures of $\mathbf{2}^{4+}$ (black) and **4** (red) in nanometre-scale MSTJ devices. In the devices at both size scales, those made from $\mathbf{2}^{4+}$ display clear hysteretic tunnelling currents and well-defined turn-on and turn-off voltages. Devices made from the two control molecules behave as classical tunnelling junctions, the only notable feature being the non-specific electric breakdown of **3** observed at −3 V. (*e*) The tunnelling current observed in the nanometre-scale MSTJ devices containing $\mathbf{2}^{4+}$ (black) over the course of 35 cycles between the switch closed (write at +2.0 V) and switch open (−2.0 V) states. Several cycles of a device incorporating **4** (red) show unchanged tunnelling current levels under the same conditions.

containing π-election-rich tetrathiafulvalene (TTF) and 1,5-dioxynaphthalene (DNP) units and terminated by bulky stoppers at each end (figure 1). Under standard conditions, the $CBPQT^{4+}$ ring in the bistable [2]rotaxane $\mathbf{1}^{4+}$ exhibits a 9 : 1 preference for encircling the TTF rather than the DNP unit. The TTF-encircled translational isomer of the bistable [2]rotaxane is therefore the ground-state co-conformation (GSCC) and its free energy is 1.8 kcal mol^{-1} lower than that of the DNP-encircled isomer, the metastable state co-conformation (MSCC; Choi *et al.* 2006). The first two oxidation processes carried out on $\mathbf{1}^{4+}$ remove electrons from the TTF π-system, resulting in the sequential formation of the TTF radical cation ($TTF^{+\cdot}$) and dication (TTF^{2+}), respectively. The

coulombic repulsion between the $TTF^{+\bullet}$ and $CBPQT^{4+}$ induces the ring to move to the DNP site. When $TTF^{+\bullet}$ or TTF^{2+} is reduced back to the neutral TTF form, the molecule is captured on the GSCC : MSCC potential energy surface only as the MSCC, where it remains for a period of time determined by the energy barrier ($\Delta G^{\ddagger}$) separating the two co-conformations. Over the course of several MSCC half-lives (ranging from less than 1 s in solution to approximately 1 h in crossbar devices), the GSCC : MSCC equilibrium is re-established. The ability to switch an ensemble of bistable [2]rotaxane molecules from the equilibrium GSCC : MSCC distribution almost exclusively to the MSCC defines, respectively, the 'open' and 'closed' states of the switch, forming the basis for using these molecules in information storage.

3. Bistable [2]rotaxanes in molecular switch tunnel junctions

While the bistable [2]rotaxanes were initially designed to operate in the solution phase, the successful incorporation of these molecules into solid-state devices is a prerequisite for their use as molecular electronic components. The amphiphilic bistable [2]rotaxane $\mathbf{2}^{4+}$ (figure 2*a*) forms smooth Langmuir–Blodgett (LB) monolayers, which were transferred onto a highly doped Si electrode (Luo *et al.* 2002). A thin protective layer of Ti (2 nm) was evaporated on top of the monolayer, followed sometimes by deposition of an aluminium top layer (figure 2*b*). This basic structure is conserved for MSTJs and crossbar memory circuits over length-scales ranging from square micrometres down to approximately 225 nm^2 per crossbar in the device.

Evidence of molecular switching in MSTJs is best characterized by measuring a remnant molecular signature (Collier *et al.* 2000; Luo *et al.* 2002). This particular measurement involves applying a write voltage across the device, after which the tunnelling current is measured at +100 mV. The first measurement is taken with a write voltage of 0.0 V with the molecules in the switch-open GSCC : MSCC equilibrium state. The write voltage is increased in 40 mV steps to +2.0 V, down to −2.0 V and finally back to 0.0 V. Remnant molecular signatures (figure 2*c*,*d*) measured from MSTJs containing the amphiphilic bistable [2]rotaxane $\mathbf{2}^{4+}$ have the same qualitative features, that is, the devices remain in a low conductance state from the beginning of the remnant measurement until the write voltage increases to +2.0 V. At +2.0 V, the device switches ON, adopting a higher conductivity state. It remains in the ON state until the write voltage reaches −2.0 V, whereupon the device returns to its lower conductivity state. The ratio in conductivity between the ON and OFF states—the so-called ON/OFF ratio—for bistable [2]rotaxane, MSTJs is approximately 10. It is also important to recognize that this hysteretic current response is only observed when switchable bistable [2]rotaxanes are present in the devices. The devices based on either the analogous amphiphilic dumb bell **3**, i.e. the amphiphilic bistable [2]rotaxanes minus the $CBPQT^{4+}$ ring or in which the motion of the $CBPQT^{4+}$ ring is impeded sterically (Choi *et al.* 2006), as well as simple molecules such as eicosanoic acid **4** show no hysteresis associated with their remnant molecular signatures.

The sharp turn-on and turn-off voltages and the distinct high- and low-conductivity states observed in the remnant molecular signatures allow for predictable device operation, an important feature for construction of large memory

arrays. Bits are turned ON by the application of a +2.0 V signal and OFF by applying −2.0 V. Devices can be cycled (figure 2*e*) between the ON and OFF states more than 100 times (although 10–20 cycles is more typical) without significant deterioration of the ON/OFF current ratio.

Based on the observation of an increased tunnelling current following the application of an oxidizing voltage, we hypothesized that the GSCC serves as the 'switch-open' device state, while the MSCC is responsible for the more highly conductive 'switch closed' state. In addition to the experimental correlation of the kinetics and thermodynamics of switching in solution with those in devices, this hypothesis was supported by first-principles simulations (Deng *et al.* 2004; Jang & Goddard 2006).

Simulated current–voltage curves of the two switch states of a some what simplified bistable [2]rotaxane (figure 3*a,b*) predicted that the MSCC should be 10–100 times more conductive than the GSCC, in agreement with the experimental MSTJ results. Furthermore, calculation of the frontier molecular orbitals of the two switch states suggested a model for the higher conductivity of the MSCC (Deng *et al.* 2004). The highest occupied molecular orbital (HOMO) and lowest unoccupied molecular orbital (LUMO) of the MSCC are significantly delocalized along the length of the rotaxane molecule, whereas each of the frontier molecular orbitals of the GSCC are localized on either the TTF station or the Au electrodes (figure 3*c*). These calculations, combined with experimental observations, support the assignment of the MSCC and GSCC to the ON and OFF states, respectively, of the switch.

4. Bistable [2]rotaxane molecular memory devices

Memory circuits incorporating bistable rotaxanes into crossbar architectures were designed and fabricated. The crossbar architecture not only exhibits the highest possible bit density for an electronically addressable memory at a given pattern resolution, but it has also been noted for its defect tolerance (Heath *et al.* 1998). Simple 64-bit memory devices (figure 4*a*) were fabricated by switching bistable rotaxanes (approx. 10^8 molecules per junction) in the crosspoints of an 8×8 grid of nanowire electrodes (Luo *et al.* 2002). Each individual bit could be turned on by applying +1.0 V to a bottom wire and −1.0 V to a top wire. This delicate way of addressing the device localizes a +2.0 V potential difference in the junction of interest, while the other junctions in the device feel a maximum potential of either +1.0 or −1.0 V. One of the 16 wires in the 64-bit memory was not operational, leaving 56 remaining good bits (figure 4*b*). Using these 56 operational bits, text strings in ASCII code were written, stored, read and erased (figure 4*c*).

After having successfully demonstrated the molecular electronic memory in devices fabricated using lithographic patterning methods, we initiated an effort to demonstrate one of the most promising features of molecular electronics—namely, scalability down and close to molecular dimensions. Over the past few years, one of us has developed the superlattice nanowire pattern transfer (SNAP) method for the fabrication of ultradense nanowire arrays (Melosh *et al.* 2003). The SNAP method has been used to pattern high quality metal or semiconductor nanowires at nanowire width and pitch as small as 8 and 16 nm, respectively. The development of techniques for fabrication, doping and reactive ion etching of

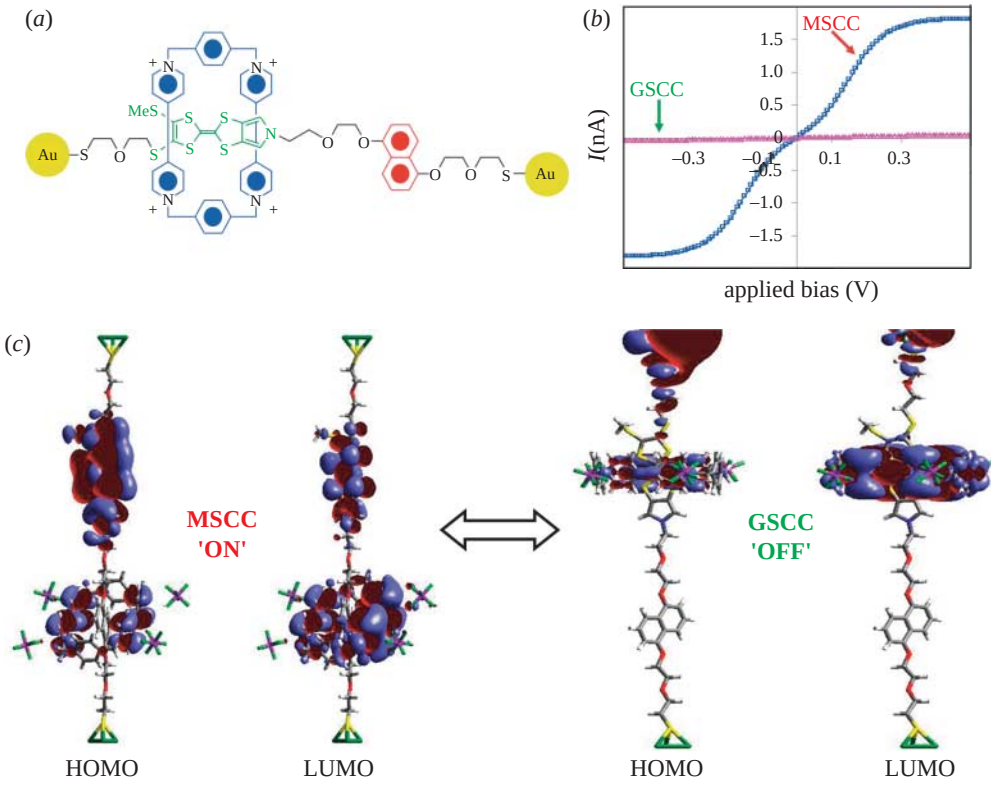

Figure 3. (*a*) Structural formula of the bistable [2]rotaxane used in the current–voltage simulations. Three Au atoms were placed at either end as model gold electrodes. (*b*) Simulated current–voltage curves of this molecule agree with the experimental observation that the MSCC is significantly more conductive than the GSCC. (*c*) Frontier molecular orbitals of both the MSCC and the GSCC. In the MSCC, both the HOMO and LUMO are delocalized along the length of the molecule, which facilitate tunnelling through the molecular switch. In contrast, the frontier molecular orbitals of the GSCC are localized on either the TTF (LUMO) or the electrodes (HOMO), making this switch state more resistive.

these systems, resulting in arrays of Si nanowires with bulk-like conductivity (figure 5*a*) ideally suited for ultradense molecular electronic memory, have been reported (Beckman *et al.* 2004).

A 4.5 kbit memory was fabricated with a bistable [2]rotaxane assembled between bottom Si and top Ti/Al nanowires, each fabricated using the SNAP technique (figure 5*b*; Beckman *et al.* 2006). Each junction of the circuit is 10×40 nm in width, affording an area that includes approximately 300 molecules per junction. Though one of us has developed novel and defect-tolerant strategies for multiplexing and demultiplexing individual SNAP wires (Beckman *et al.* 2005), for simplicity, this 4.5 kbit memory was tested by contacting three or four nanowires simultaneously. Of the 64 effective bits tested in this memory, roughly half worked and these working bits showed qualitatively similar behaviour to that of lower density memory devices. This first demonstration of a working ultradense memory indicates that these devices may be successfully scaled to junctions containing a very small number of molecules. Our most recent efforts have yielded the successful

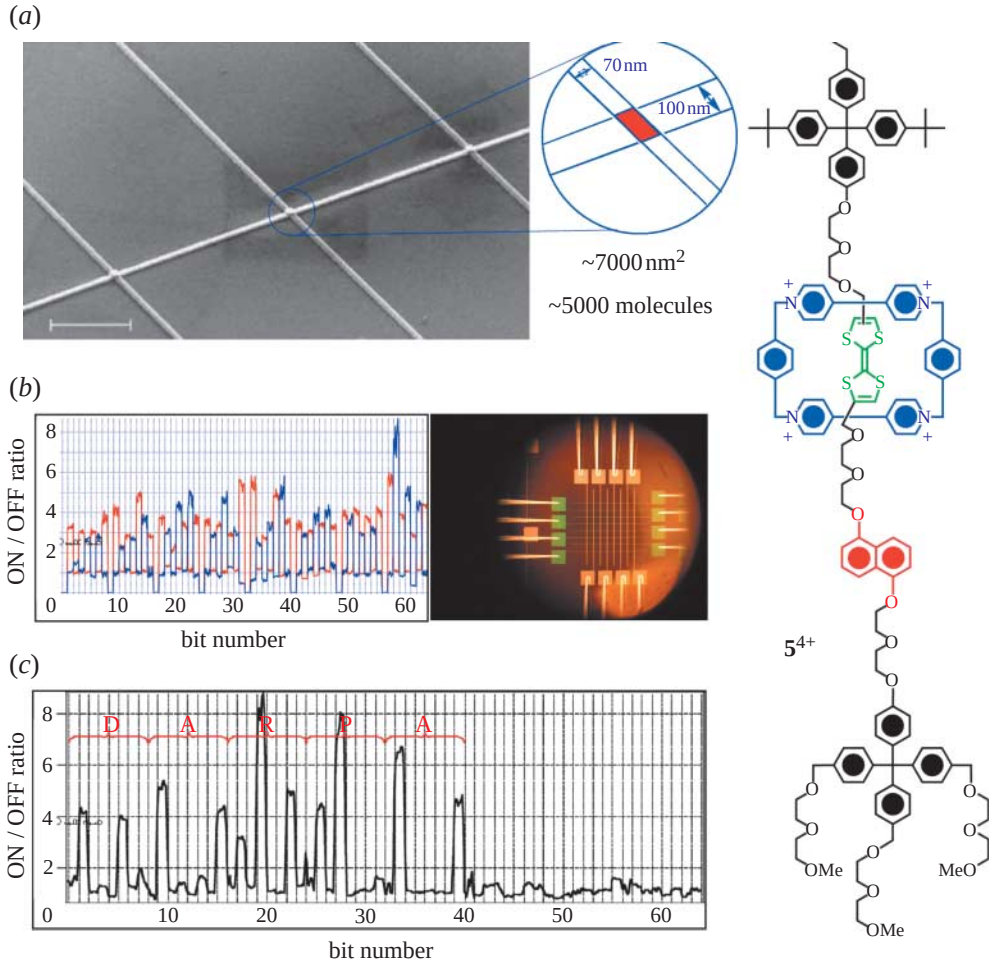

Figure 4. (*a*) A scanning electron microscope (SEM) image of the nanowire crossbars fabricated by e-beam lithography. The width of the wires and the active device area are shown in the inset. The amphiphilic bistable [2]rotaxane $\mathbf{5}^{4+}$ is assembled between horizontal and vertical wires. Scale bar, 2 μm. (*b*) 56 of the 64 bits in the array gave ON/OFF ratios of 2 : 1 or greater. (*c*) The acronym 'DARPA' was stored in ACSII within the memory.

demonstration of a 160 kbit memory at 10^{11} bits cm^{-2} (Green *et al.* 2007), a density which correlates to the 2028 node of the International Technology Roadmap for Semiconductors published in 2005.

5. Kinetic and thermodynamics of bistable [2]rotaxane switching across different environments

A major goal in the field of molecular electronics is to develop the ability to manipulate device properties predictably through chemical synthesis and solution-state characterization. With the intention from the outset of addressing this challenge, we undertook a major effort to correlate the switching mechanism

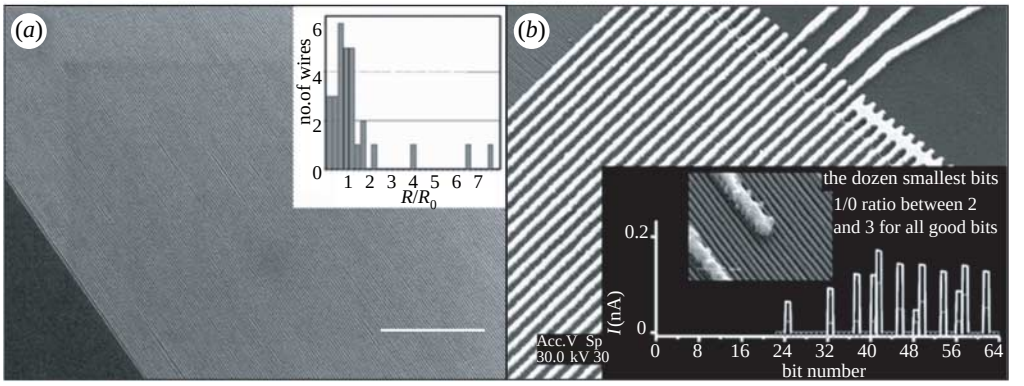

Figure 5. (*a*) Parallel Si nanowires were patterned from a Si (111) on insulator (SOI) substrate using the SNAP technique. The wires are 15 nm in diameter, 30 nm tall and 3 mm in length. Inset: a histogram of the electrical characteristics of the nanowires indicates that they are essentially bulk-like, and with few defects. R_0 is the calculated resistivity of the nanowires based on the doping level of the SOI substrate and R is the measured resistivity of the nanowire. A large majority of the nanowires tested show conductivity close to that predicted from their doping level. Scale bar, 2 μm. (*b*) An electron micrograph of a 4.5 kbit memory device consisting of a monolayer of $\mathbf{5}^{4+}$ sandwiched between 10 nm wide Si bottom nanowires and 40 nm wide Ti/Al top nanowires. Each junction contains approximately 300 rotaxane molecules. Inset: each of the electrical contacts to the Si nanowires, patterned by electron-beam lithography, touches 3–4 nanowires. The ON and OFF currents of 13 of the smallest 24 bits is shown.

of bistable [2]rotaxanes in solution with their behaviour in other more device-relevant environments—for example, in self-assembled monolayers (SAMs; Tseng *et al.* 2004*b*), viscous polymer gels (Steuerman *et al.* 2004) and MSTJs (Choi *et al.* 2006). These investigations convincingly confirmed that a universal switching mechanism operates across all environments. This important demonstration and realization also suggest key design parameters for developing new molecular switches for use in any device setting.

Kinetic and thermodynamic parameters were measured for three different bistable [2]rotaxanes (figure 6). Compounds $\mathbf{5}^{4+}$ and $\mathbf{6}^{4+}$ contain the same 'simple' TTF primary binding site with diethyleneglycol spacers between the TTF and DNP units, and each exhibit a 1 : 9 equilibrium MSCC : GSCC ratio. Compound $\mathbf{7}^{4+}$ contains a bispyrrolotetrathiafulvalene (BPTTF) unit as the electrochemically active binding site and, since the $CBPQT^{4+}$ ring exhibits a weaker preference for binding the BPTTF relative to the DNP unit, the equilibrium ratio for MSCC : GSCC falls to 1 : 4 at 288 K. Compounds $\mathbf{5}^{4+}$ and $\mathbf{7}^{4+}$ each contains hydrophilic stoppers for incorporation into MSTJs as LB monolayers. In compound $\mathbf{6}^{4+}$, the hydrophilic stopper is replaced by the one bearing a benzylic alcohol function, which serves as a handle to allow it to be incorporated into other device settings.

(*a*) *Solution phase*

The first oxidation of the TTF units in the bistable [2]rotaxane is highly sensitive to the location of the $CBPQT^{4+}$ ring, permitting a determination of the MSCC : GSCC ratio by cyclic voltammetry (CV; Flood *et al.* 2004). As a result, the thermodynamic parameters for the starting-state equilibrium have been

determined by carrying out a series of variable time and temperature cyclic voltammetry (VTTCV) measurements. For example, the solution phase CV of the bistable [2]rotaxane $\mathbf{7}^{4+}$ (figure 7) contains a peak at +530 mV, which corresponds to the first oxidation of the BPTTF unit from that part of the equilibrium population of molecules, which are already in the MSCC. The next oxidation peak centred on +680 mV corresponds to the first oxidation of the BPTTF units in the GSCC. The second oxidation of the BPTTF unit at +780 mV is not a reflection of the initial GSCC : MSCC ratio because the $CBPQT^{4+}$ ring moves to the DNP site after the first electron has been removed from the TTF π-system. This measurement of the equilibrium GSCC : MSCC ratio was carried out as a function of temperature. For $\mathbf{7}^{4+}$, the MSCC : GSCC ratio increased from 0.3 to 0.7 as the temperature was decreased from 284 K down to 262 K. In contrast, the MSCC : GSCC ratios for the $\mathbf{5}^{4+}$ bearing the simple TTF units did not change significantly from 0.1 over a broad temperature range (248–283 K).

These sharply contrasting responses to temperature change correspond remarkably well to the thermodynamic binding parameters as measured by isothermal titration calorimetry between the host **CBPQT**·$4PF_6$ and a diethyleneglycol-functionalized DNP derivative and very similar TTF derivatives as guests (Choi *et al.* 2006). On the other hand, the binding of the $\mathbf{CBPQT}^{4+}$ host to the BPTTF-containing guest, relative to that of the DNP-containing guest, exhibit a high enthalpy difference—a factor which leads to temperature-sensitive equilibria—the binding of guests containing TTF relative to those containing DNP exhibit almost no difference in enthalpy, resulting in a switch whose equilibrium ratio is not highly temperature dependent. The ability to design temperature-independent molecular switches based on binding data obtained from small model compounds is an important objective in molecular electronics, simply because most applications require consistent operation over a wide range of temperatures.

The kinetic barrier to relaxation from the MSCC to the steady-state equilibrium was also measured in solution by VTTCV by collecting two consecutive CV scans, beginning with the molecules in the GSCC (Flood *et al.* 2004; Choi *et al.* 2006). The first scan gives information about the MSCC : GSCC equilibrium ratio. If, however, the second scan is collected before the system re-establishes the steady-state equilibrium, it will show an area-enhanced oxidation peak for the MSCC. By performing this measurement at different scan rates, a measure of the rate of relaxation of the MSCC to the GSCC is obtained, and the full characterization of this behaviour over a range of temperatures allows quantification of the activation barrier using the Eyring relationship. $\mathbf{5}^{4+}$ and $\mathbf{7}^{4+}$ exhibited barriers to relaxation ($\Delta G^{\ddagger}_{298}$) of 16.2 and 17.7 kcal mol^{-1}, respectively. These values correspond to a MSCC solution half-life (τ_{298}) ranging from 1.2 s for $\mathbf{7}^{4+}$ to 0.123 s for $\mathbf{5}^{4+}$.

(*b*) *Self-assembled monolayers on gold*

An investigation of the switching processes experienced by a bistable [2]rotaxane assembled onto gold electrode 'half-devices' represents a key step in the understanding of the behaviour of molecular switches when they are assembled into 'full-devices' containing both top and bottom electrodes (Tseng *et al.* 2004*b*). A derivative of the bistable [2]rotaxane $\mathbf{6}^{4+}$ (figure 8), capable of forming SAMs on Au, was prepared by functionalizing the benzylic alcohol group at the smaller of the two stoppers with a disulphide tether. VTTCV experiments, similar to these described for

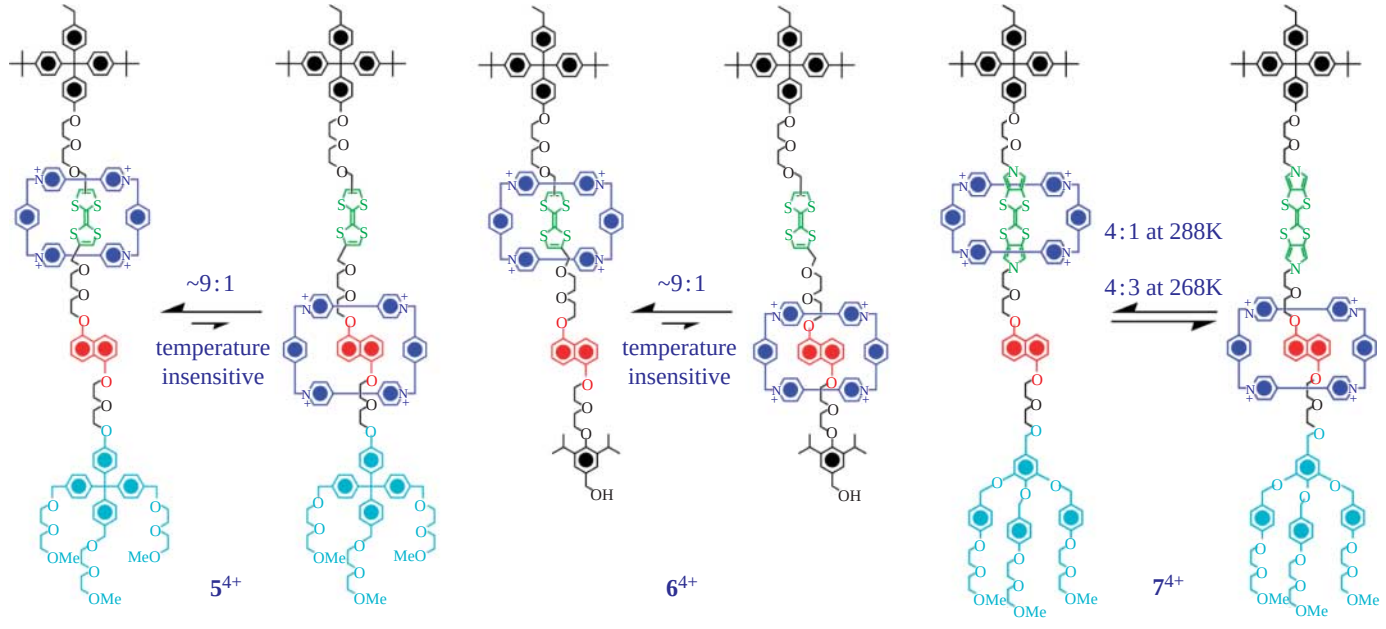

Figure 6. Structural formulae of the translational isomers of the bistable [2]rotaxanes used for kinetic and thermodynamic studies across a variety of chemical environments. All of the tetracationic bistable [2]rotaxanes discussed in this work were isolated and characterized as their tetrakis(hexaflourophosphate) salts.

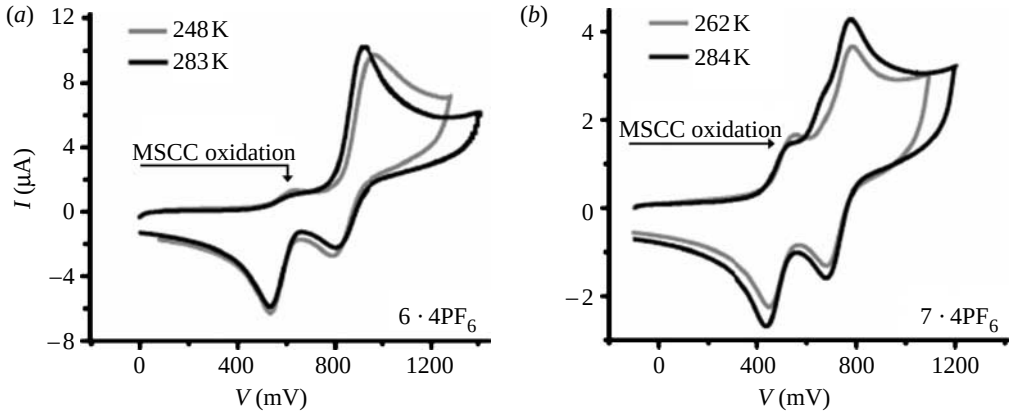

Figure 7. Cyclic voltammetry of (*a*) $\mathbf{6}^{4+}$ and (*b*) $\mathbf{7}^{4+}$ obtained from solutions of the rotaxanes initially at translational equilibrium. The magnitude of the MSCC oxidation peak remains fairly constant over a 35°C range for $\mathbf{6}^{4+}$, whereas the MSCC oxidation peak seen from $\mathbf{7}^{4+}$ increases in intensity upon cooling 22°C.

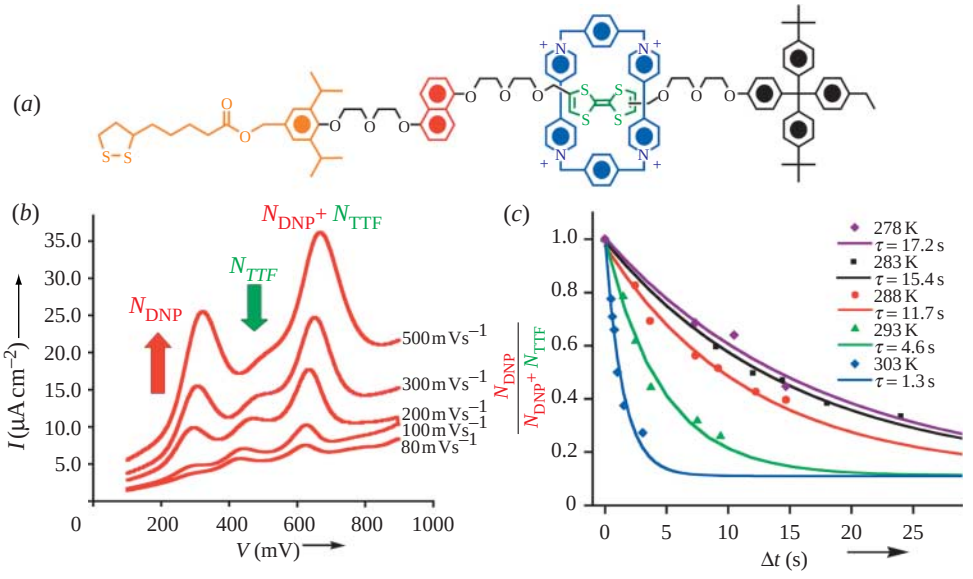

Figure 8. (*a*) Structure of a switchable bistable [2]rotaxane derivative of $\mathbf{6}^{4+}$ that forms SAMS on gold surfaces. (*b*) The cathodic peaks of the second CV cycles measured at various scan rates at 288 K. The fraction of molecules remaining in the MSCC increases with increased scan rate, as observed by the enhanced oxidation peak at +310 mV. (*c*) The relaxation decay of the MSCC isomer over a range of different temperatures. This process was modelled as a thermally activated first-order decay, with an activation energy calculated from an Arrhenius plot (E_a) of 17.7 ± 2.8 kcal mol^{-1}.

solution-phase measurements, were performed using a standard three-electrode temperature-controlled cell with a SAM-functionalized Au working electrode. Significantly, the initial CV scans of the SAMs showed an identical MSCC : GSCC equilibrium ratio (approx. 0.1) as those of $\mathbf{5}^{4+}$ in solution. This ratio was also shown

to be relatively insensitive to temperature, suggesting that the thermodynamic aspects of the molecular switch are unchanged in the half-device format.

The barrier to relaxation in the SAMs was determined by quantifying the MSCC : GSCC ratio over a range of different scan rates and temperatures (Tseng *et al.* 2004*b*). The appearance of (i) a strongly enhanced MSCC oxidation peak, (ii) the disappearance of the GSCC oxidation peak, and (iii) the time-dependent re-equilibration of the solution and surface-bound bistable molecules suggest strongly that the switching mechanism observed in solution is also operating in the SAM environment. The relaxation barrier ($\Delta G^{\ddagger}_{298}$) calculated from an Eyring plot of the rate of MSCC relaxation as a function of temperature was 17.8 kcal mol^{-1}, corresponding to a τ_{293} of 4.6 s, that is, roughly two orders of magnitude longer than the lifetime of the MSCC of $\mathbf{5}^{4+}$ in solution.

(*c*) *Polymer matrices*

The two states of the redox-controllable bistable [2]rotaxanes containing CBPQT^{4+} encircling TTF and DNP units differ in colour on account of the green CBPQT^{4+}/TTF charge-transfer interaction in the GSCC and the red CBPQT^{4+}/DNP charge-transfer interaction in the MSCC. Hence, bistable [2]rotaxanes, dispersed in a polymer electrolyte gel, form the basis for a two-colour electrochromic device (figure 9*a–c*; Steuerman *et al.* 2004). It is this device setting that has inspired subsequent synthetic and theoretical efforts to design tristable systems, capable of displaying red, green and blue from a single molecular switch (Deng *et al.* 2005). The kinetics and thermodynamics of the switching process in these polymer matrices are of both mechanistic and practical interests, since key device metrics, such as the intensity and the speed of the colour change, depend on these parameters.

The polymer matrix (MeCN/poly(methyl methacrylate)/propylene carbonate/$LiClO_4$, 70 : 7 : 20 : 7) is 10 000 times more viscous than the MeCN solvent used for the solution measurements. Not surprisingly, the viscous media presents an increased barrier to shuttling, namely 18.1 kcal mol^{-1} for $\mathbf{5}^{4+}$ and 19.4 kcal mol^{-1} for $\mathbf{7}^{4+}$, again resulting in MSCC lifetimes at least two orders of magnitude longer than those observed in solution. These changes are consistent with what would be expected from Kramers' theory (Kramers 1940). Despite the increased barrier to relaxation to the GSCC, the ground-state thermodynamics were unaffected by the polymer matrix. For $\mathbf{5}^{4+}$, each of the VTTCV initial scans taken at different temperatures showed the same 10 : 1 preference for the GSCC as observed in solution. By contrast, the MSCC : GSCC equilibrium ratio for $\mathbf{7}^{4+}$ remained quite temperature sensitive in the polymer environment. This phenomenon is also apparent in MSCC decay profiles (figure 9*e*) as the decay approaches asymptotically higher MSCC : GSCC equilibrium ratios at lower temperatures.

(*d*) *Molecular switch tunnel junctions*

The position of the MSCC : GSCC equilibrium and barrier to MSCC relaxation are both extremely important parameters in MSTJ memory devices. A low preference for the GSCC or highly temperature-dependent equilibrium would lead to poor or thermally unstable ON/OFF ratios. Furthermore, the retention time of the memory is directly related to the barrier of MSCC

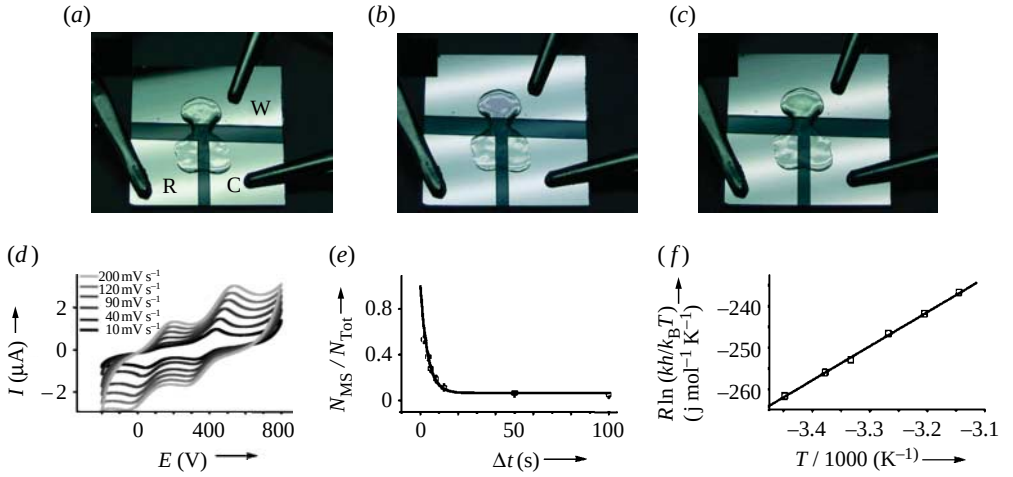

Figure 9. (*a–c*) Operation of an electrochromic polymer device based on bistable [2]rotaxane $\mathbf{6}^{4+}$. The working (W), counter (C) and reference (R) electrodes are indicated in (*a*). (*a*) The device at zero bias and the molecules in the GSCC : MSCC equilibrium. (*b*) A +1 V potential has been applied across the device, causing oxidation of the TTF followed by translational isomerization. Returning the device back to zero bias generates the metastable state of $\mathbf{6}^{4+}$, causing the polymer matrix to appear red. (*c*) Several seconds after the working electrode has been returned to zero bias, $\mathbf{6}^{4+}$ has relaxed back to the GSCC : MSCC equilibrium, regenerating the original green colour. (*d–f*) Experimental data used to extract the kinetic parameters of the MSCC→GSCC relaxation process of $\mathbf{6}^{4+}$ within the solid-state polymer electrolyte environment. (*d*) A series of second scan CVs recorded at 296 K at various scan rates. The intensity of the first oxidation wave is indicative of the MSCC population. (*e*) The population ratios of the MSCC and the relaxation times fit well to a first-order decay model. (*f*) The temperature dependence of the relaxation kinetics expressed as an Eyring plot.

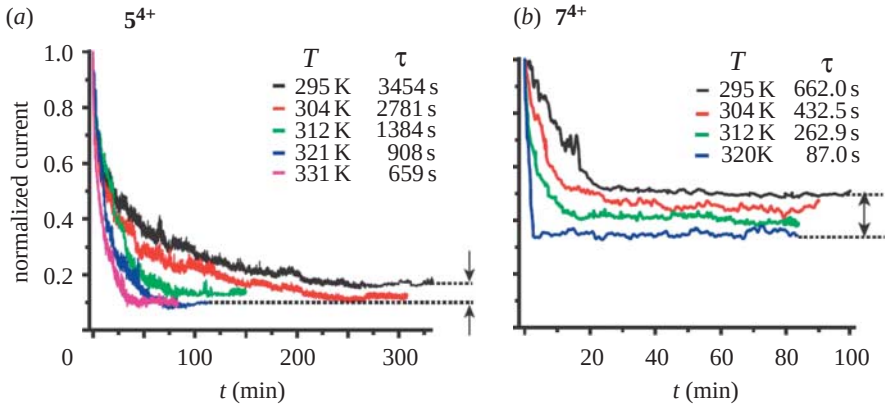

Figure 10. Decay curves of the high conductivity state of MSTJ devices containing (*a*) $\mathbf{5}^{4+}$ and (*b*) $\mathbf{7}^{4+}$, respectively, recorded over a range of temperatures. The significant temperature dependence of the GSCC : MSCC equilibrium in $\mathbf{7}^{4+}$ is again observed. The MSTJs containing $\mathbf{7}^{4+}$ decay to widely differing equilibrium current ratios at different temperatures, following the trend observed for these molecules in solution.

relaxation. Correlation of these parameters in the MSTJ device environment to molecular properties in solution will provide design principles for future MED applications.

Since CV measurements cannot be performed on MSTJs, other electronic probes of the MSCC : GSCC ratio in real time are required. Based on the fact that the MSCC exhibits a higher tunnelling conductivity than the GSCC, the MSCC relaxation can be probed by switching the device to its high-conductance state and measuring the rate of decay back to the low-conductance state (figure 10; Choi *et al.* 2006). The temperature dependence of the MSCC decay rate allows the calculation of $\Delta G^{\ddagger}$ and τ by the same methods as employed in the VTTCV measurements. Decay curves for both $\mathbf{5}^{4+}$ and $\mathbf{7}^{4+}$, obtained by this method, clearly show that the relaxation back to the low-current state is an activated process similar to that observed in other environments. However, with a τ_{295} of 3450 s for $\mathbf{5}^{4+}$ and 660 s for $\mathbf{7}^{4+}$, the MSTJs are nearly three orders of magnitude slower than those observed for SAMs and polymer gels, reflecting the sterically restricted MSTJ environment. Furthermore, despite the difficulty of quantifying the position of the MSCC : GSCC equilibrium in MSTJs, trends in changes of the ON/OFF ratio as a function of temperature can be correlated to the quantitative data obtained in other environments.

6. Structural characterization of [2]rotaxane Langmuir–Blodgett films

In order to gain a more complete understanding of the behaviour of bistable [2]rotaxanes in MSTJs, the superstructures of amphiphilic bistable [2]rotaxane LB monolayers were investigated by both theoretical and experimental methods. Molecular dynamics simulations, performed on bistable [2]rotaxane molecules at the air–water interface, showed an increase in the thickness of the LB monolayer as the area per molecule was decreased, indicating that the molecules are tilted considerably with respect to the water surface until increasing the pressure on the Langmuir trough forces them to stand up (Jang *et al.* 2005*a*). Interestingly, the LB monolayer thicknesses were found to be similar for both co-conformations. Thus, switching of the bistable [2]rotaxanes between the GSCC and the MSCC does not require significant reorganization of the monolayer. A similar trend was also noted in simulations of bistable [2]rotaxanes as SAMs on Au surfaces (Jang *et al.* 2005*b*).

Calculations of the overall tilt angle of the bistable [2]rotaxane molecules as a function of packing area also support the situation wherein the molecules stand up straighter as they are forced to pack more closely. They also suggest that the overall tilt angle is independent of co-conformation. Interestingly, calculations of individual tilt angles for the two different recognition sites (TTF and DNP) in the [2]rotaxane LB monolayer indicate that the site encircled by the $CBPQT^{4+}$ ring has a small tilt angle, whereas the free site adopts a folded conformation even in tightly packed films.

The simulated LB monolayer systems were used to calculate electron density profiles as a function of area per molecule. Impressively, these theoretical electron density profiles agree extremely well with those measured experimentally by X-ray reflectometry, providing physical confirmation of the above calculations (Norgaard *et al.* 2005*a*). In subsequent X-ray reflectometry

Table 1. Peak assignments for FT-RAIRS.

	118 Å^2/molecule		73 Å^2/molecule		54 Å^2/molecule	
assignment	bare ML	ML w/2 nm Ti	bare ML	ML w/2 nm Ti	bare ML	ML w/2 nm Ti
C–H stretch (–CH3)	2966, 2873	2873 (shoulder)	2967, 2871	2964 (shoulder)	2966, 2873	2873
C–H stretch (–CH2–)	2928, 2910	2930, 2859	2930, 2906	2930, 2859	2930, 2909	2930, 2859
C=C bend of phenyl rings	1608, 1507, 1493, 1457	none	1609, 1508, 1491, 1457	1608, 1508, 1492, 1457	1608, 1510, 1492, 1457	1608, 1510, 1492, 1457
C–O–C stretch	1250	1250	1252	1252	1250	1250

measurements, the electron density of the film was measured both before and after addition of an oxidant to the subphase (figure 11; Norgaard *et al.* 2005*b*). The 1.2 nm vertical shift in electron density observed in these experiments is attributed to the movement of the $CBPQT^{4+}$ ring from the oxidized TTF site to the DNP one. This vertical shift was observed in two different constitutionally isomeric [2]rotaxane systems (figure 11*b*). When the TTF unit, encircled by the $CBPQT^{4+}$ ring ($\mathbf{8}^{4+}$), was closer to the hydrophobic stopper, addition of oxidant resulted in movement of electron density towards the water surface (figure 11*c*). The constitutional isomer with the TTF encircled by the $CBPQT^{4+}$ ring closer to the hydrophilic stopper ($\mathbf{9}^{4+}$) exhibited movement of electron density away from the water surface (figure 11*d*). Molecular modelling estimates the TTF–DNP distance in an extended conformation of the molecule to be 37 Å, further supporting the notion that the rotaxane molecules are somewhat contorted in the LB monolayer environment. Additional experimental studies on Langmuir films of amphiphilic rotaxanes have elucidated the role of structural modifications of the hydrophilic stoppers to film packing (Lee *et al.* 2004).

Finally, a very recent investigation sheds light on how deposition of a top Ti electrode affects the integrity of the switching gear in the monolayers of the bistable [2]rotaxanes assembled using the LB technique (DeIonno *et al.* 2006). Bistable [2]rotaxane monolayers were transferred onto patterned poly Si at three different packing densities (118, 73 and 54 Å^2 per molecule) and characterized by Fourier transform reflection absorption infrared spectroscopy (FT-RAIRS). The spectra were measured again after the deposition of a 2 nm thick film of Ti, and the switching characteristics of subsequent fully fabricated devices were also measured. By checking the properties through this sequence of experiments, it was possible to determine which portions of the bistable [2]rotaxane molecules were damaged by the Ti evaporation process and correlate these changes with device performance. The outcome of all this careful work is that the switching gear survives the fabrication process owing to the protective role played by the hydrophobic stoppers.

Monolayers which were transferred at 73 Å^2 per molecule—the optimum packing density for MSTJ performance—showed changes primarily to the C–H stretches of the *tert*-butyl groups in the hydrophobic stopper after Ti deposition

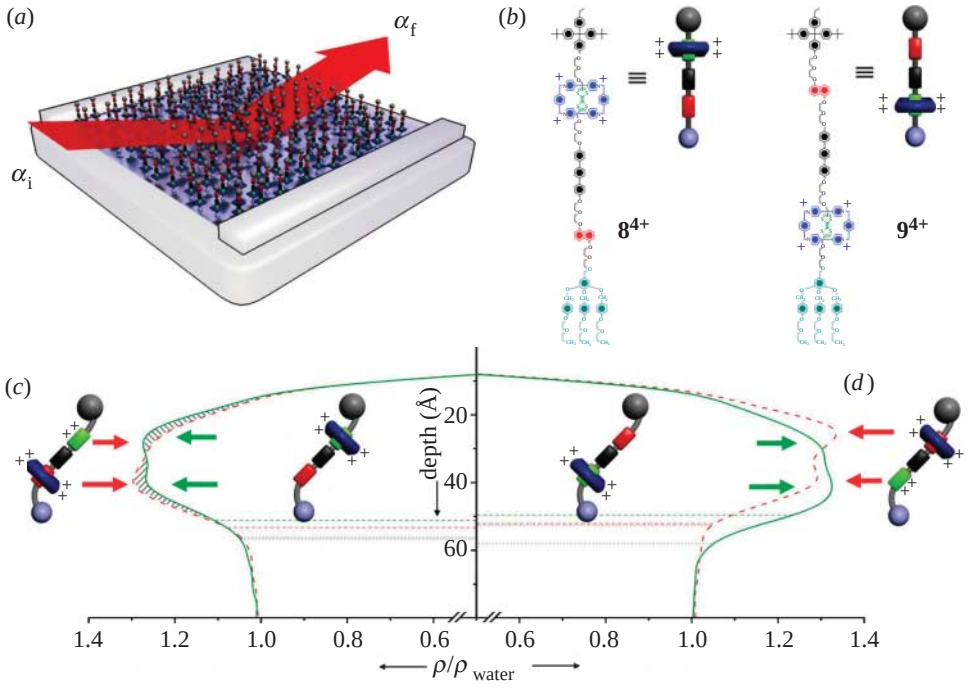

Figure 11. (*a*) A schematic of the working principle in specular X-ray reflectivity measurements of Langmuir monolayers. The incident (α_i) and exit grazing angle (α_f) of the X-ray radiation (red arrow) are varied simultaneously ($\alpha_f = \alpha_i$) while recording the intensity pattern that results from the interference of X-rays reflected from different depths of the sample. (*b*) Graphical representation and structural formulae of the amphiphilic bistable [2]rotaxanes $\mathbf{8}^{4+}$ and $\mathbf{9}^{4+}$. (*c*, *d*) Electron density profiles for (*c*) $\mathbf{8}^{4+}$ and (*d*) $\mathbf{9}^{4+}$, respectively, inverted from the reflectivity data for the tetracationic starting compounds (green lines) and the *in situ* oxidized hexacationic compounds generated by adding $Fe(ClO_4)_3$ to the subphase (red lines). The areas above the horizontal dashed lines correspond to the numbers of electrons in one molecule, while the dotted lines represent the approximate position of the interface to bulk water.

(table 1; figure 12*b*). Absorbances corresponding to other parts of the molecule, such as C–H stretches arising from the methylene groups in the glycol chains and the C=C phenyl ring bend, were mostly unaffected. As expected, these devices showed good hysteresis upon switching and ON/OFF ratios similar to those in devices studied previously (figure 12*d*–*e*). While monolayers transferred at 54 $Å^2$ per molecule gave very similar results (figure 12*c*), the devices showed reduced switching amplitude which can be attributed to increased steric interactions in the more tightly packed film. By contrast, monolayers transferred at 118 $Å^2$ per molecule showed significant changes throughout their FT-RAIRS spectra after Ti deposition (figure 12*a*), strongly suggestive of non-specific damage to the molecules. The switching characteristics of these devices confirmed this hypothesis. No clear current hysteresis was observed in the least closely packed monolayers. All of these observations indicate that, in tightly packed LB films, the bulky tetraarylmethane stoppers form a protective barrier that shields the functional portion of the molecules from damage during Ti deposition. These

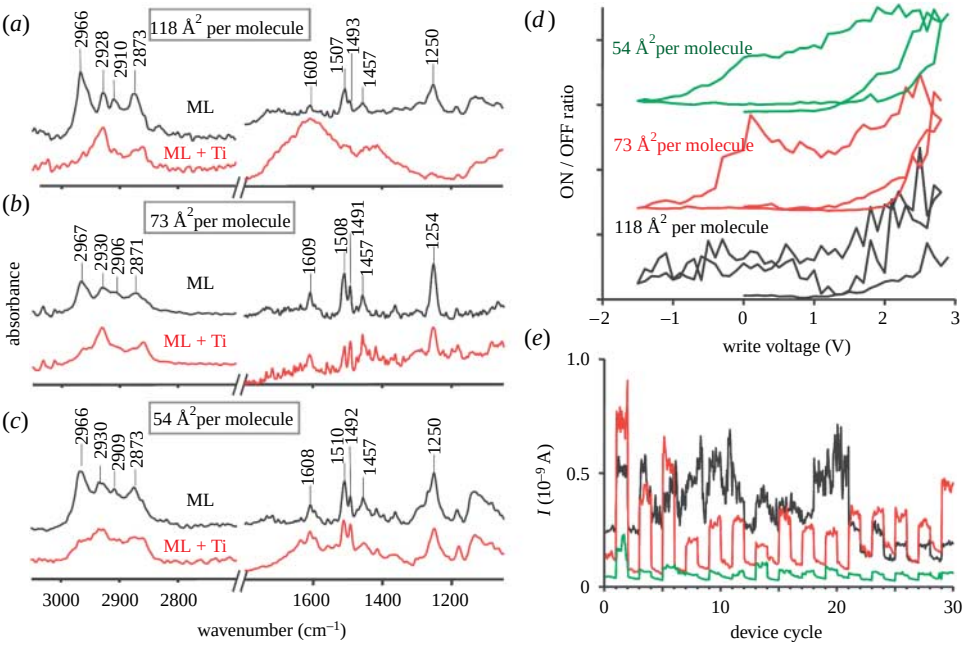

Figure 12. (*a–c*) FT-RAIRS spectra of bistable [2]rotaxane monolayers transferred at (*a*) 118 Å^2 per molecule, (*b*) 73 Å^2 per molecule and (*c*) 54 Å^2 per molecule, respectively, taken both before (black) and after (red) deposition of a 2 nm Ti film. (*d*) Remnant hysteresis plots for MSTJ devices incorporating bistable [2]rotaxane LB monolayers transferred at the same packing densities. (*e*) Cycling data for these devices. Both remnant and cycling data show that devices prepared from LB monolayers transferred at the two higher packing densities exhibit approximately the same switching amplitudes, although the current magnitude for the 54 Å^2 per molecule MSTJ is significantly less than that for the 73 Å^2 per molecule MSTJ. The devices prepared from LB monolayers at 118 Å^2 per molecule do not show good switching behaviour in the remnant scan or the cycling tests.

observations provide further confirmation that bistable [2]rotaxane molecules remain functional during the MSTJ fabrication process and emphasize the importance of the bulky stoppers, as well as well-packed monolayers in the fabrication of MEDs of this type.

7. Conclusions and outlook

By integrating electrochemically switchable bistable [2]rotaxanes into nanowire crossbar arrays, large memory devices of unprecedented density were fabricated and successfully operated. Careful theoretical calculations and characterization of the rotaxane LB monolayers and solid-state devices gave insight into the structure of the molecules in the device format. The hysteretic changes in tunnelling current that form the basis of memory device operation were shown to originate directly from the electromechanical switching process of the bistable [2]rotaxanes. By correlating the kinetic and thermodynamic properties of the switching process in solution with that observed across many condensed environments, a universal switching mechanism was shown to be operable. By establishing this important

feedback loop between solution and device behaviour, we now believe it is possible to design new molecules for use as electronic components or in nanoelectromechanical systems using the tools of chemical synthesis, a goal that embodies one of the great promises of molecular nanotechnology.

The authors acknowledge the many stimulating discussions and intellectual contributions of our former and current colleagues whose names appear in the references. This research has been supported by grants from the Defense Advanced Research Projects Agency (DARPA) and both the Functional Engineered Nano Architectonics (FENA) Focus Center and the Center for Advanced Materials and Devices within the Microelectronics Advanced Research Corporation (MARCO).

References

Anelli, P.-L. *et al.* 1992 Molecular meccano. 1. [2]Rotaxanes and a [2]catenane made to order. *J. Am. Chem. Soc.* **114**, 193–218. (doi:10.1021/ja00027a027)

Balzani, V., Credi, A., Mattersteig, G., Matthews, O. A., Raymo, F. M., Stoddart, J. F., Venturi, M., White, A. J. P. & Williams, D. J. 2000 Switching of pseudorotaxanes and catenanes incorporating a tetrathiafulvalene unit by redox and chemical inputs. *J. Org. Chem.* **65**, 1924–1936. (doi:10.1021/jo991781t)

Beckman, R. A., Johnston-Halperin, E., Melosh, N. A., Luo, Y., Green, J. E. & Heath, J. R. 2004 Fabrication of conducting Si nanowire arrays. *J. Appl. Phys.* **96**, 5921–5923. (doi:10.1063/1.1801155)

Beckman, R., Johnston-Halperin, E., Luo, Y., Green, J. E. & Heath, J. R. 2005 Bridging dimensions: demultiplexing ultrahigh-density nanowire circuits. *Science* **310**, 465–468. (doi:10.1126/science.1114757)

Beckman, R. *et al.* 2006 Molecular mechanics and molecular electronics (Spiers Memorial Lecture). *Farad. Discuss.* **131**, 9–22. (doi:10.1039/b513148k)

Bissell, R. A., Cordova, E., Kaifer, A. E. & Stoddart, J. F. 1994 A chemically and electrochemically switchable molecular shuttle. *Nature* **369**, 133–137. (doi:10.1038/369133a0)

Choi, J. W. *et al.* 2006 Ground-state equilibrium thermodynamics and switching kinetics of bistable [2]rotaxanes switched in solution, polymer gels, and molecular electronic devices. *Chem. Eur. J.* **12**, 261–279. (doi:10.1002/chem.200500934)

Collier, C. P., Mattersteig, G., Wong, E. W., Luo, Y., Beverly, K., Sampaio, J., Raymo, F. M., Stoddart, J. F. & Heath, J. R. 2000 A [2]catenane-based solid state electronically reconfigurable switch. *Science* **289**, 1172–1175. (doi:10.1126/science.289.5482.1172)

Collier, C. P., Jeppesen, J. O., Luo, Y., Perkins, J., Wong, E. W., Heath, J. R. & Stoddart, J. F. 2001 Molecular-based electronically switchable tunnel junction devices. *J. Am. Chem. Soc.* **123**, 12 632–12 641. (doi:10.1021/ja0114456)

DeIonno, E., Tseng, H.-R., Harvey, D. D., Stoddart, J. F. & Heath, J. R. 2006 Infrared spectroscopic characterization of [2]rotaxane molecular switch tunnel junction devices. *J. Phys. Chem. B* **110**, 7609–7612. (doi:10.1021/jp0607723)

Deng, W. Q., Muller, R. P. & Goddard, W. A. 2004 Mechanism of the Stoddart–Heath bistable rotaxane molecular switch. *J. Am. Chem. Soc.* **126**, 13 562–13 563. (doi:10.1021/ja036498x)

Deng, W. Q., Flood, A. H., Stoddart, J. F. & Goddard, W. A. 2005 An electrochemical color-switchable RGB dye: tristable [2]catenane. *J. Am. Chem. Soc.* **127**, 15 994–15 995. (doi:10.1021/ja0431298)

Diehl, M. R., Steuerman, D. W., Tseng, H.-R., Vignon, S. A., Star, A., Celestre, P. C., Stoddart, J. F. & Heath, J. R. 2003 Single-walled carbon nanotube based molecular switch tunnel junctions. *ChemPhysChem* **4**, 1335–1339. (doi:10.1002/cphc.200300871)

Flood, A. H., Peters, A. J., Vignon, S. A., Steuerman, D. W., Tseng, H.-R., Kang, S., Heath, J. R. & Stoddart, J. F. 2004 The role of physical environment on molecular electromechanical switching. *Chem. Eur. J.* **10**, 6558–6564. (doi:10.1002/chem.200401052)

Green, J. E. *et al.* 2007 A 160-kilobit molecular electronic memory patterned at 10^{11} bits per square centimetre. *Nature* **445**, 414–417. (doi:10.1038/nature05462)

Heath, J. R., Kuekes, P. J., Snider, G. S. & Williams, R. S. 1998 A defect-tolerant computer architecture: opportunities for nanotechnology. *Science* **280**, 1716–1721. (doi:10.1126/science.280.5370.1716)

Jang, Y. H. & Goddard, W. A. 2006 Mechanism of oxidative shuttling for [2]rotaxane in a Stoddart–Heath molecular switch: density functional theory study with continuum-solvation model. *J. Phys. Chem. B* **110**, 7660–7665. (doi:10.1021/jp055473c)

Jang, S. S. *et al.* 2005*a* Molecular dynamics simulation of amphiphilic bistable [2]rotaxane Langmuir monolayers at the air/water interface. *J. Am. Chem. Soc.* **127**, 14 804–14 816. (doi:10.1021/ja0531531)

Jang, S. S. *et al.* 2005*b* Structures and properties of self-assembled monolayers of bistable [2]rotaxanes on Au(111) surfaces from molecular dynamics simulations validated with experiment. *J. Am. Chem. Soc.* **127**, 1563–1575. (doi:10.1021/ja044530x)

Kramers, H. A. 1940 Brownian motion in a field of force and the diffusion model of chemical reactions. *Physica* **7**, 284–304. (doi:10.1016/S0031-8914(40)90098-2)

Lee, I. C., Frank, C. W., Yamamoto, T., Tseng, H.-R., Flood, A. H., Stoddart, J. F. & Jeppesen, J. O. 2004 Langmuir and Langmuir–Blodgett films of amphiphilic bistable rotaxanes. *Langmuir* **20**, 5809–5828. (doi:10.1021/la0361518)

Lehn, J.-M. 1995 *Supramolecular chemistry.* Weinheim, Germany: VCH.

Luo, Y. *et al.* 2002 Two-dimensional molecular electronics circuits. *Chem. Phys. Chem.* **3**, 519–525. (doi:10.1002/1439-7641(20020617)3:6<519::AID-CPHC519>3.0.CO;2-2)

Melosh, N. A., Boukai, A., Diana, F., Gerardot, B., Badolato, A., Petroff, P. M. & Heath, J. R. 2003 Ultrahigh-density nanowire lattices and circuits. *Science* **300**, 112–115. (doi:10.1126/science.1081940)

Norgaard, K., Jeppesen, J. O., Laursen, B. A., Simonsen, J. B., Weygand, M. J., Kjaer, K., Stoddart, J. F. & Bjornholm, T. 2005*a* Evidence of strong hydration and significant tilt of amphiphilic [2]rotaxane molecules in langmuir films studied by synchrotron X-ray reflectivity. *J. Phys. Chem. B* **109**, 1063–1066. (doi:10.1021/jp0448494)

Norgaard, K., Laursen, B. W., Nygaard, S., Kjaer, K., Tseng, H.-R., Flood, A. H., Stoddart, J. F. & Bjornholm, T. 2005*b* Structural evidence of mechanical shuttling in condensed monolayers of bistable rotaxane molecules. *Angew. Chem. Int. Ed.* **44**, 7035–7039. (doi:10.1002/anie.200501538)

Steuerman, D. W., Tseng, H.-R., Peters, A. J., Flood, A. H., Jeppesen, J. O., Nielsen, K. A., Stoddart, J. F. & Heath, J. R. 2004 Molecular-mechanical switch-based solid-state electrochromic devices. *Angew. Chem. Int. Ed.* **43**, 6486–6491. (doi:10.1002/anie.200461723)

Tseng, H.-R. & Stoddart, J. F. 2002 Chemical synthesis gets a fillip from molecular recognition and self-assembly processes. *Proc. Natl Acad. Sci. USA* **99**, 4797–4800. (doi:10.1073/pnas.052708999)

Tseng, H.-R. *et al.* 2004*a* Redox-controllable amphiphilic [2]rotaxanes. *Chem. Eur. J.* **10**, 155–172. (doi:10.1002/chem.200305204)

Tseng, H.-R., Wu, D. M., Fang, N. X. L., Zhang, X. & Stoddart, J. F. 2004*b* The metastability of an electrochemically controlled nanoscale machine on gold surfaces. *Chem. Phys. Chem.* **5**, 111–116. (doi:10.1002/cphc.200300992)